

CORONAL COMPOSITION MEASUREMENT

Slimane MZERGUAT

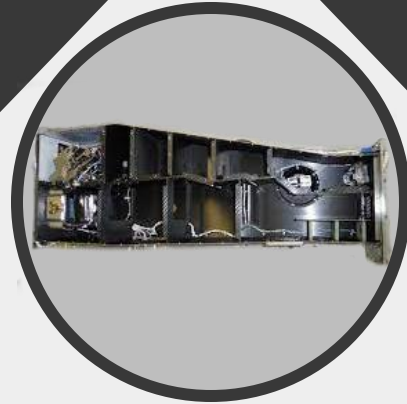
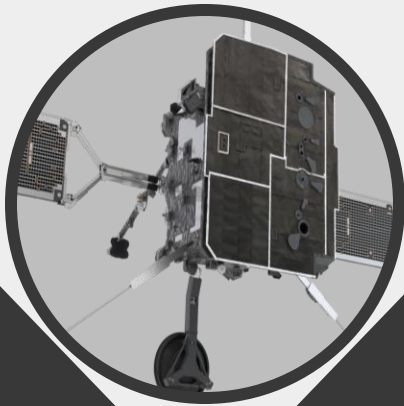
Eric BUCHLIN
Miho JANVIER

A multi-instrumental analysis including Solar Orbiter/SPICE
Institut d'Astrophysique Spatiale (IAS),
France

PNST 2024

SOLAR ORBITER

Joint ESA-NASA mission, explores the Sun's magnetic fields, solar wind, and inner heliosphere, orbiting as close as **60 solar radii**. Equipped with **10 instruments**.



SPICE

SPICE (Spectral Imaging of the Coronal Environment) captures **EUV spectra**, providing data for plasma diagnostics from **upper chromosphere to lower corona**

SPICE INSTRUMENT

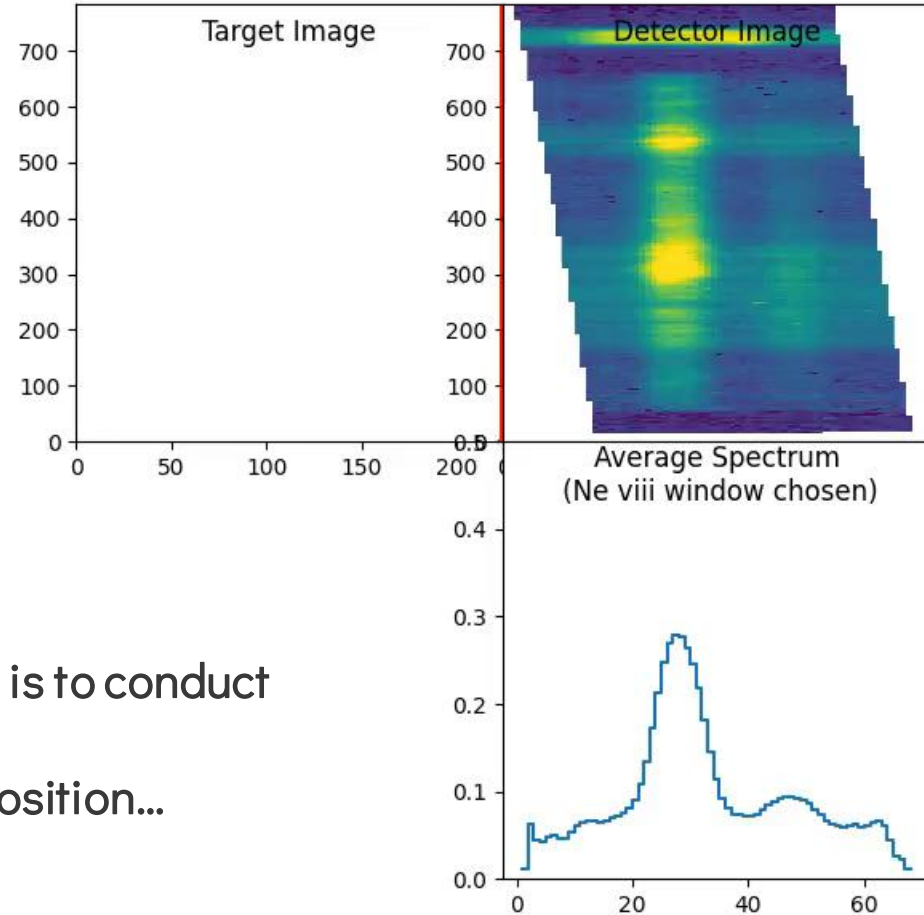
One data cube

⇒ 1 image is a set of N exposures along x direction. (can be time consuming)

⇒ 3 axes (spatial directions + spectral direction).

⇒ discrete spectral windows.

The main task for SPICE instrument is to conduct plasma diagnostics:
Temperature, Doppler, Composition...



SPICE OBSERVATIONS

The main task for SPICE Instrument is to conduct plasma diagnostics:

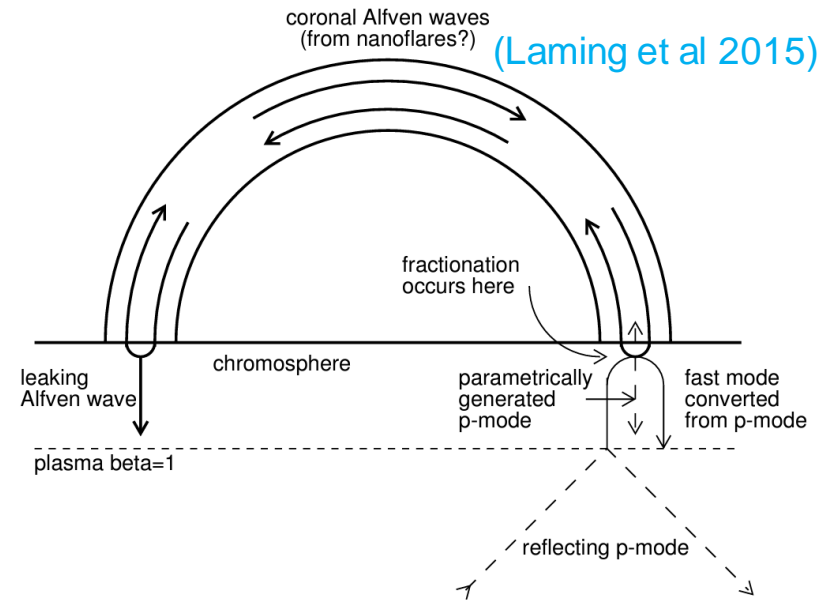
Temperature, Doppler, **Composition**

why **Composition** :

- Needed to fully describe plasma evolution.
- A tracer of the **source region** of the solar wind.
- Linked to different physical processes: Wave propagation and absorption, reconnection...

SPICE COMPOSITION

Composition



“**FIP bias**” : abundance bias as a function of the elements’ First ionization potential.

- Elements with Low FIP (LF) (<10 eV) are more enhanced (2 times or more) compared with High FIP elements
- Measured in the solar wind as well as in the corona
- See poster ([Alixis P.Rouillard, Nicolas Poirier](#))

SPICE COMPOSITION

Composition ← FIP bias

LCR method: Linear Combination Ratio

A new method for reconstructing elemental abundances using a set of lines from Low FIP (LF) elements and another from High FIP (HF) elements.

Method assumptions:

- Transparent plasma (doesn't work in filaments)
- LF and HF combinations of lines have close contribution functions

(Zambrana Prado et.al 2019)

SPICE COMPOSITION

Composition ← FIP Bias ← LCR methods

SAFFRON: Spectral Analysis, Fitting Framework, Reduction Of Noise.

- A local pipeline for fitting SPICE L2 data and providing plasma diagnostics.
 - Automatic initial parameter generator.
 - Denoising
 - Despiking (Cosmics...)
 - Convolution (for increasing signal power)
 - Fitting and error estimation ... etc.

SPICE COMPOSITION

Composition ← FIP Bias ← LCR methods ← SAFFRON

SAFFRON: Spectral Analysis, Fitting Framework, Reduction Of Noise.

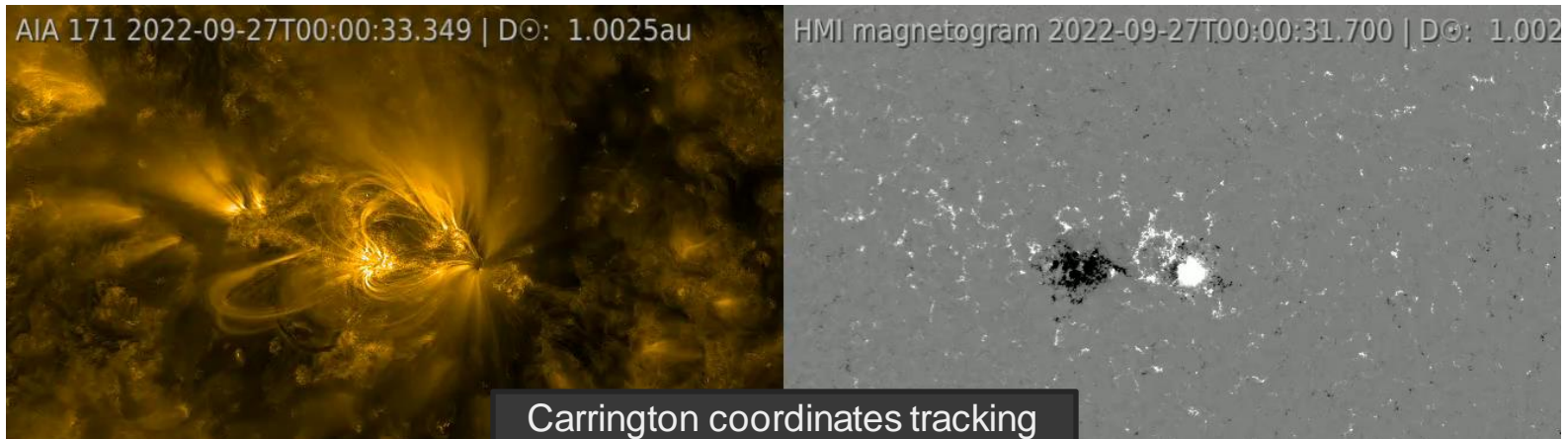
- A local pipeline for fitting SPICE L2 data and providing plasma diagnostics.
 - Automatic initial parameter generator.
 - Denoising
 - Despiking (Cosmics...)
 - Convolution (for increasing signal power)
 - Fitting and error estimation ... etc.

OBSERVATIONAL CONTEXT

It all started with an active region...

AR13110

Facing earth between 27-09-2022 and 05-10-2022

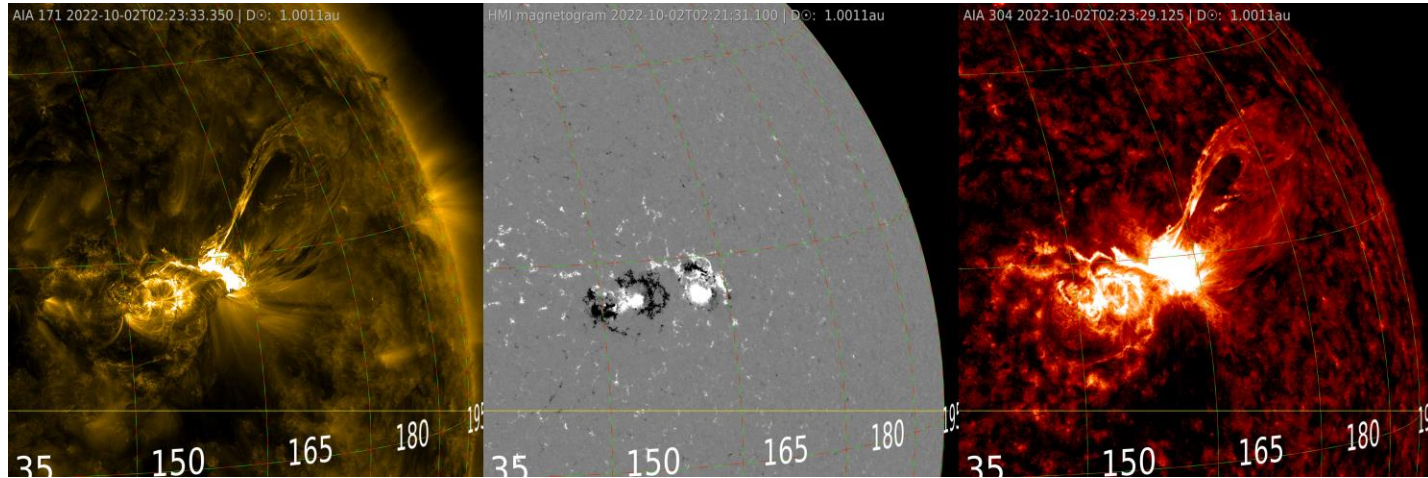


OBSERVATIONAL CONTEXT

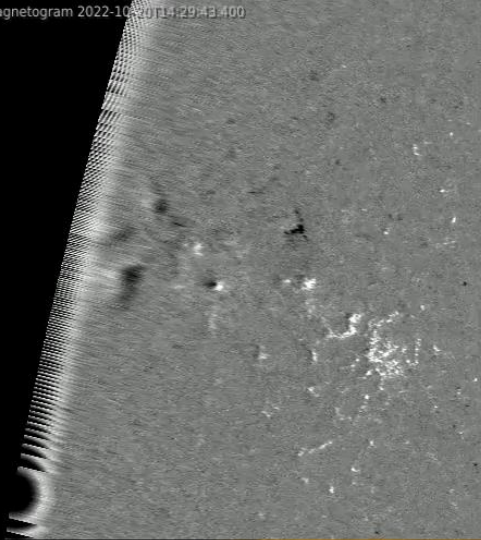
Multiple events on AR13110

X1.0 flare on 2-10-2022, peak at 20:25 UTC.
M5.86 flare on 1-10-2022, peak at 20:10 UTC.
CME on 2-10-2022 around 02:00 UTC.

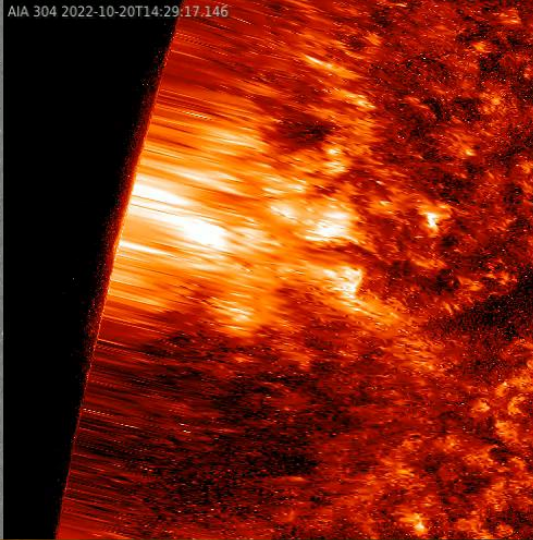
Good target for
AR decaying study
SOOP: AR long term
tracking



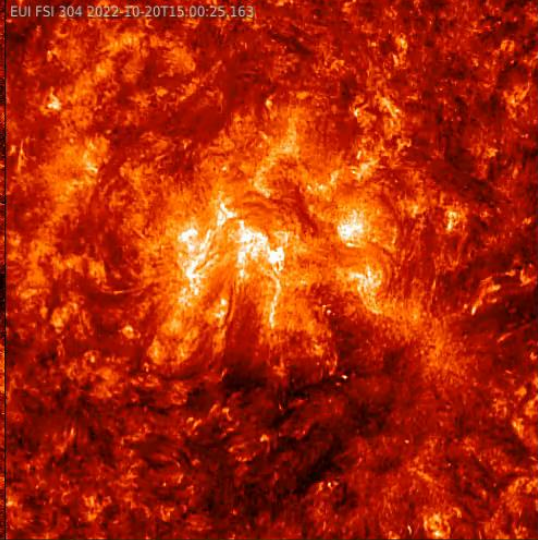
HMI magnetogram 2022-10-20T14:29:43.400



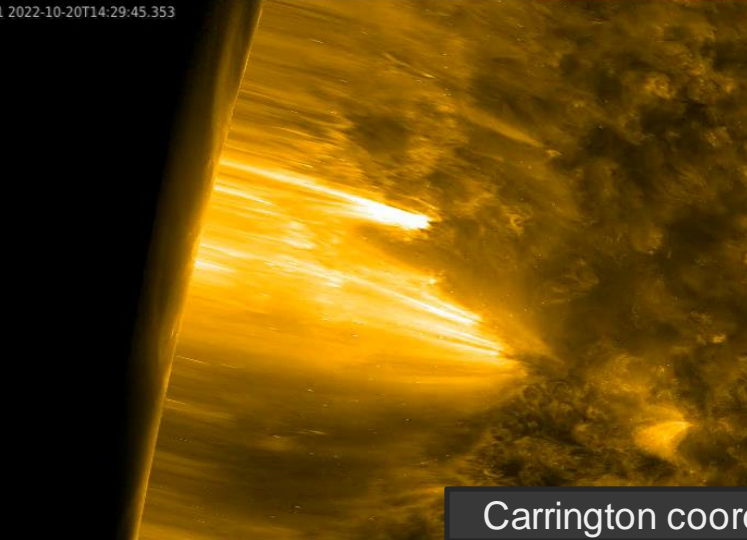
AIA 304 2022-10-20T14:29:17.146



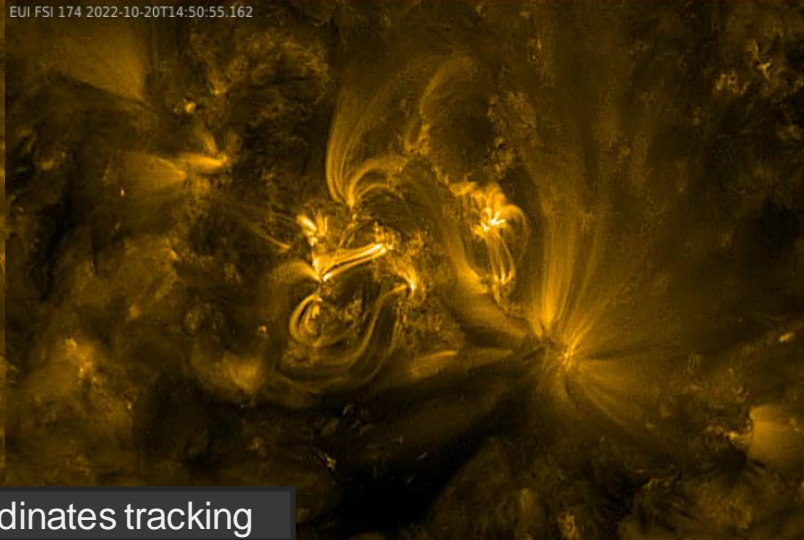
EUI FSI 304 2022-10-20T15:00:25.163



AIA 171 2022-10-20T14:29:45.353

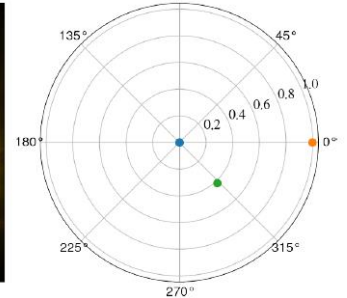
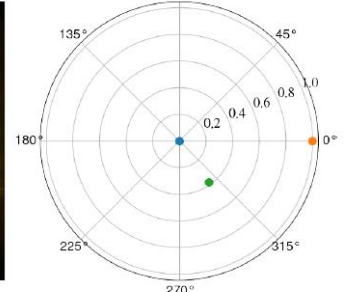
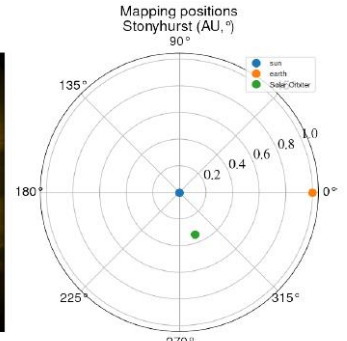
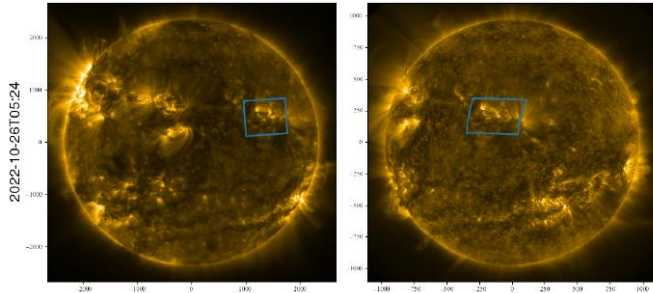
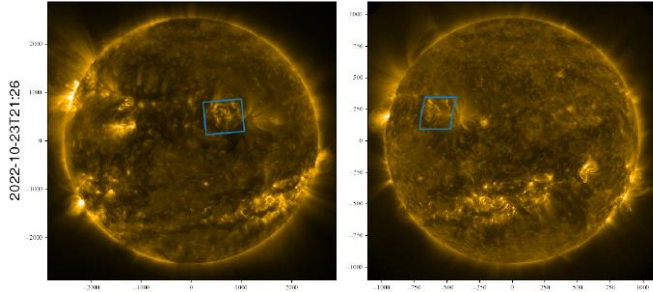
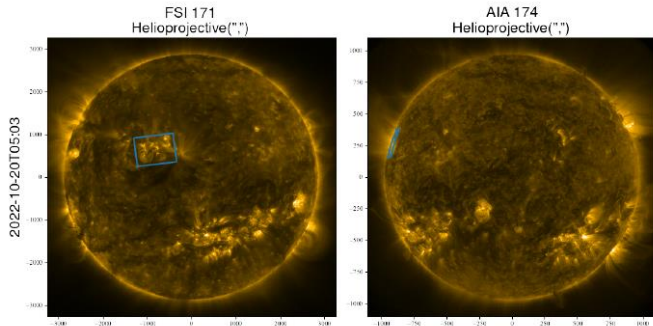


EUI FSI 174 2022-10-20T14:50:55.162



Carrington coordinates tracking

OBSERVATIONAL CONTEXT

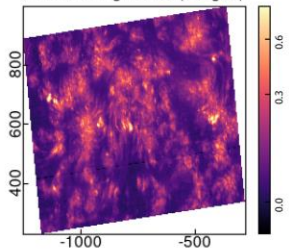


SPICE DATA

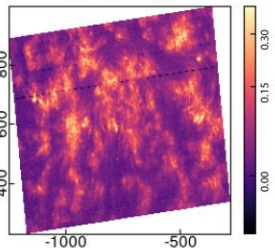
2022-10-20T03:16:03.983

L2 data spectral average

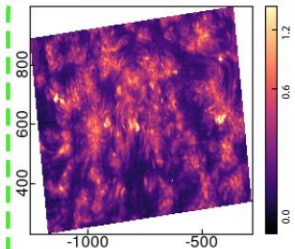
O III 703 / Mg IX 706 (Merged)



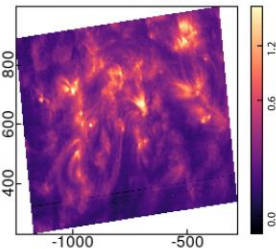
S IV 750 - Peak



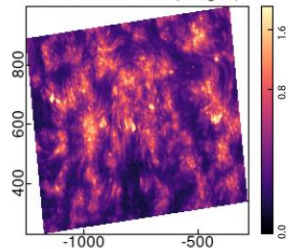
N IV 765 - Peak



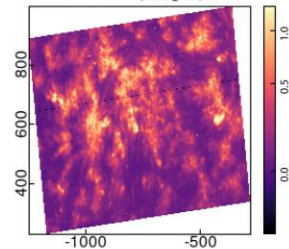
Ne VIII 770 - Peak



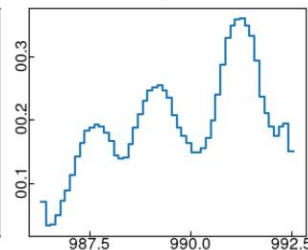
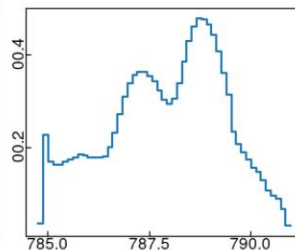
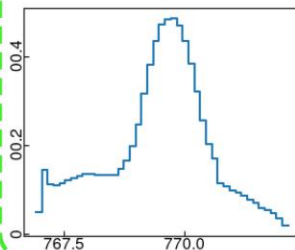
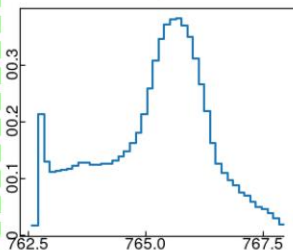
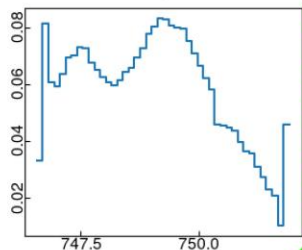
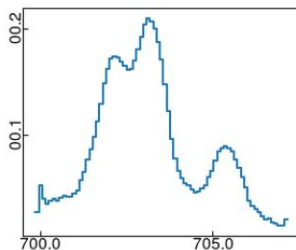
S V 786 / O IV 787 (Merged)



N III 991 (Merged)



L2 data spatial average



O III-(702.33Å &
702.89Å & 702.82Å),
O III-(703.87Å),
Mg IX-(706.02Å)

S IV-(748.40Å),
Mg IX-(749.54Å),
S IV-(750.22Å)

N IV-(765.15Å)

Ne VIII-(770.42Å)

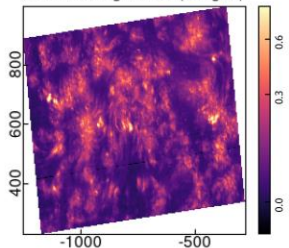
S V-(786.47Å),
O IV-(787.72Å)

Na VI-(988.65Å),
O I-(988.75 Å),
N III-(989.82Å),
N III-(991.59Å)

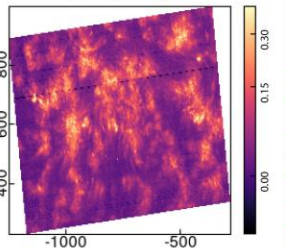
2022-10-20T03:16:03.983

L2 data spectral average

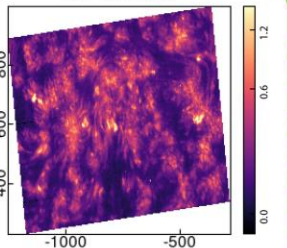
O III 703 / Mg IX 706 (Merged)



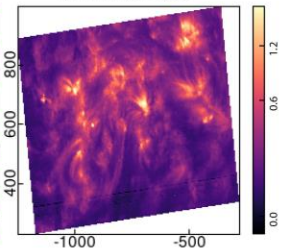
S IV 750 - Peak



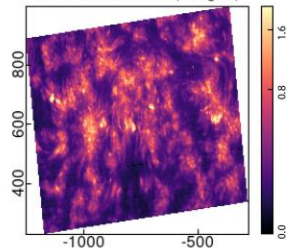
N IV 765 - Peak



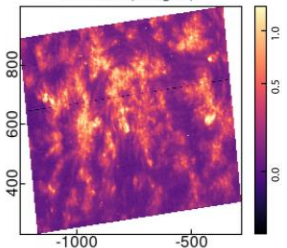
Ne VIII 770 - Peak



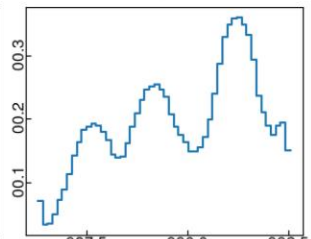
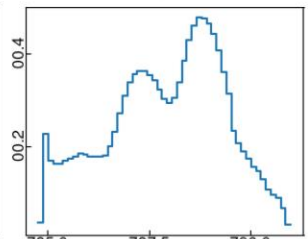
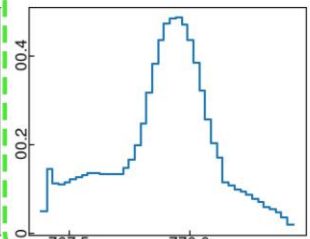
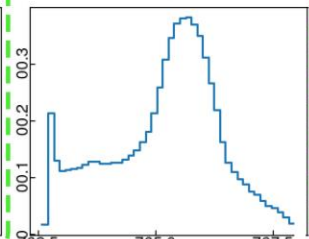
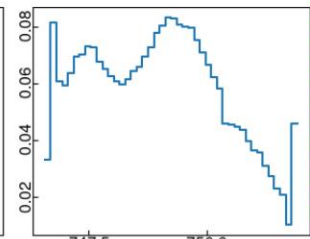
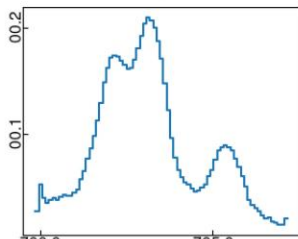
S V 786 / O IV 787 (Merged)



N III 991 (Merged)

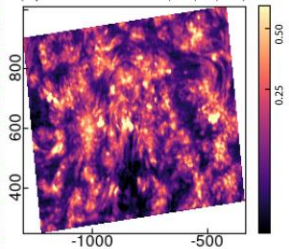


L2 data spatial average

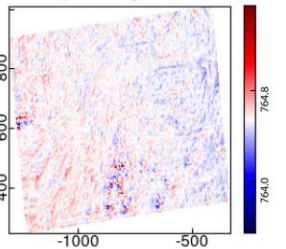


N iv Parameters and uncertainties

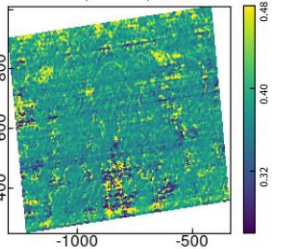
I_{Niv}
(Spectral radiance $W/m^2/s^2/sr$)



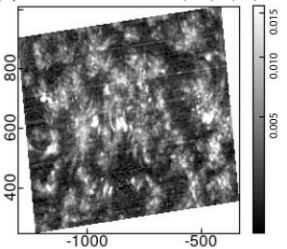
λ_{Niv}
(Wavelength \AA)



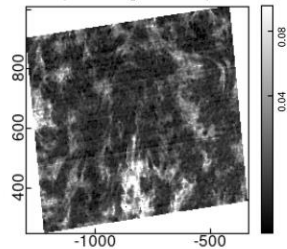
σ_{Niv}
(Width \AA)



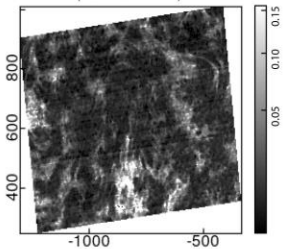
ΔI_{Niv}
(Spectral radiance error $W/m^2/s^2/sr$)

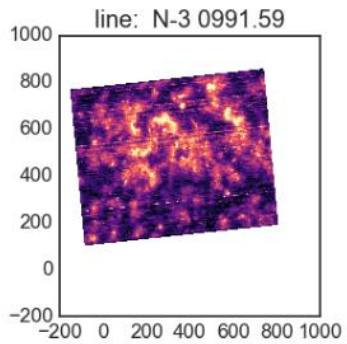
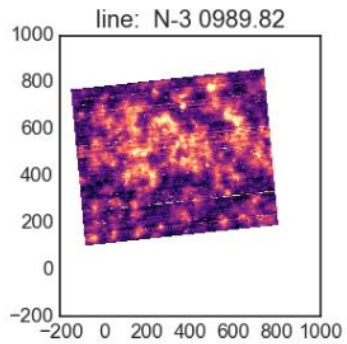
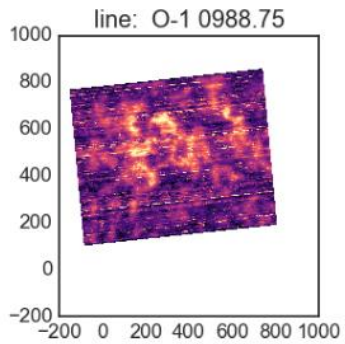
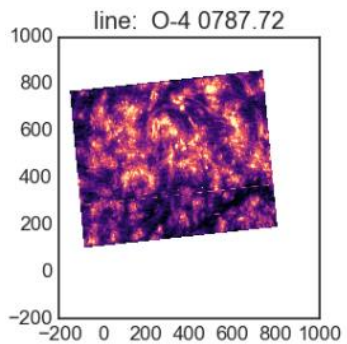
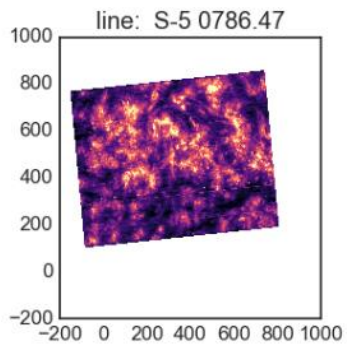
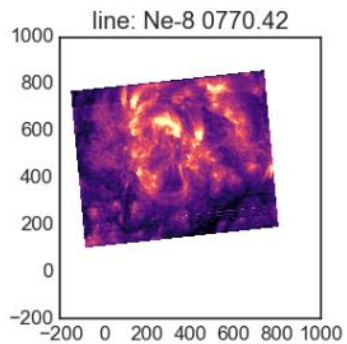
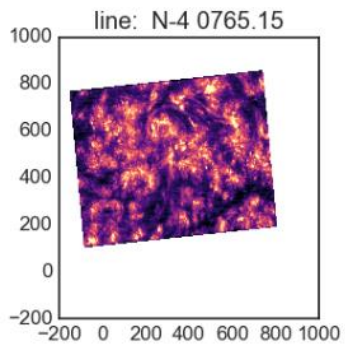
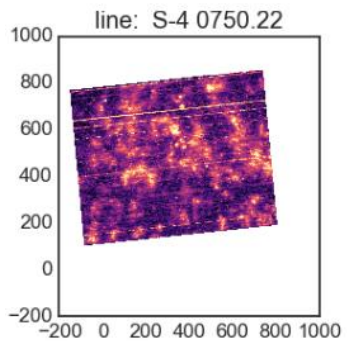
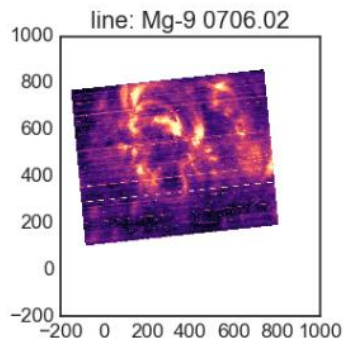
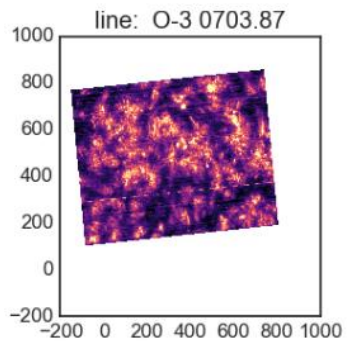
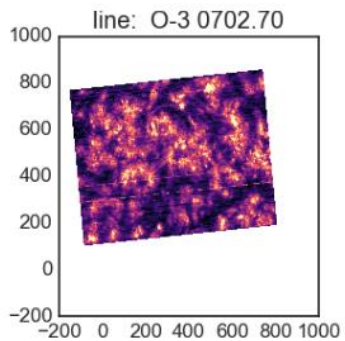


$\Delta \lambda_{Niv}$
(Wavelength error \AA)

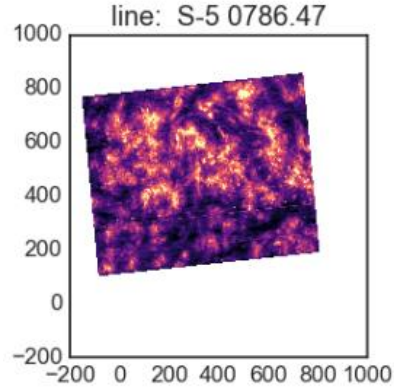
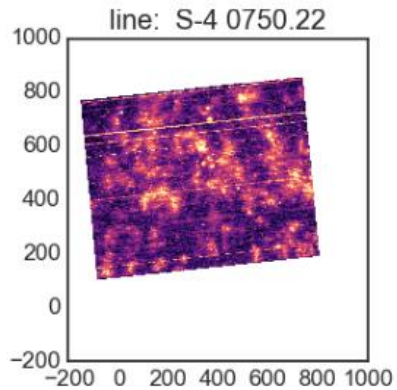


$\Delta \sigma_{Niv}$
(Width error \AA)

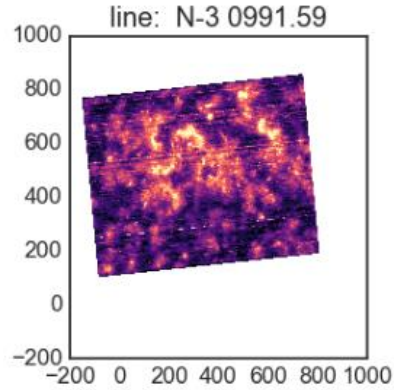
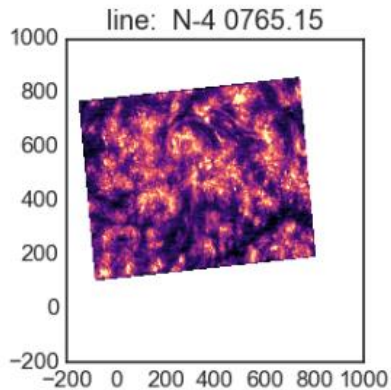




SPICE DATA

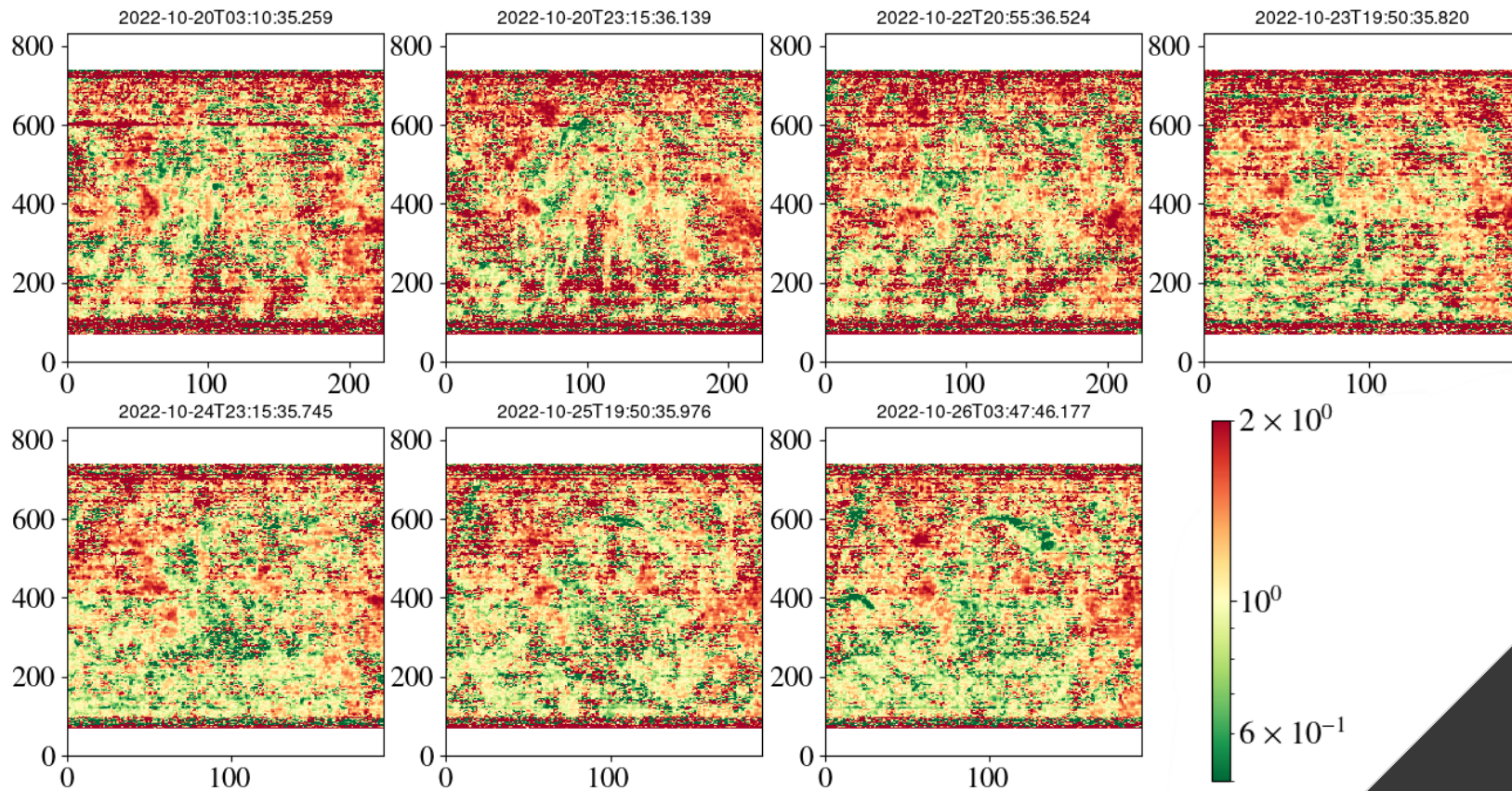


Low FIP lines

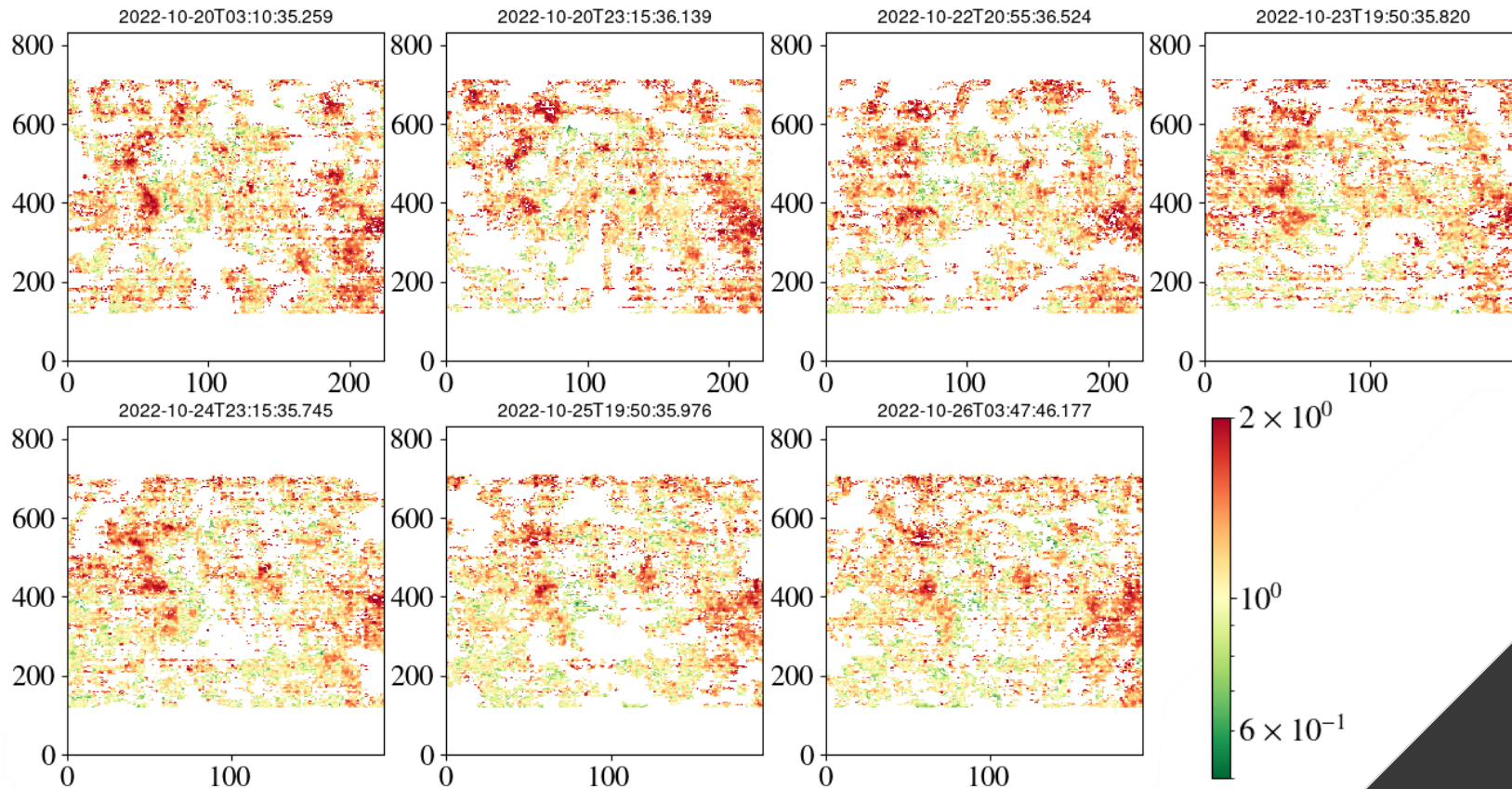


High FIP lines

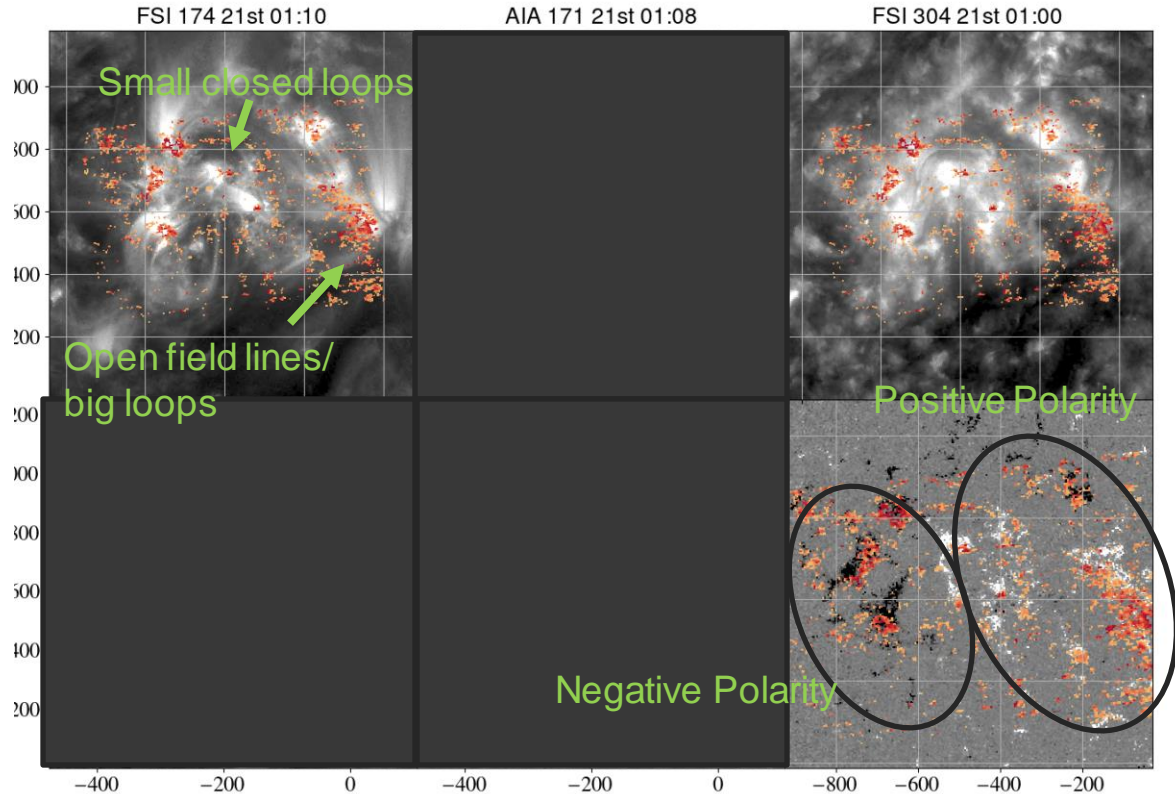
COMPOSITION MAPS (RAW RESULTS)

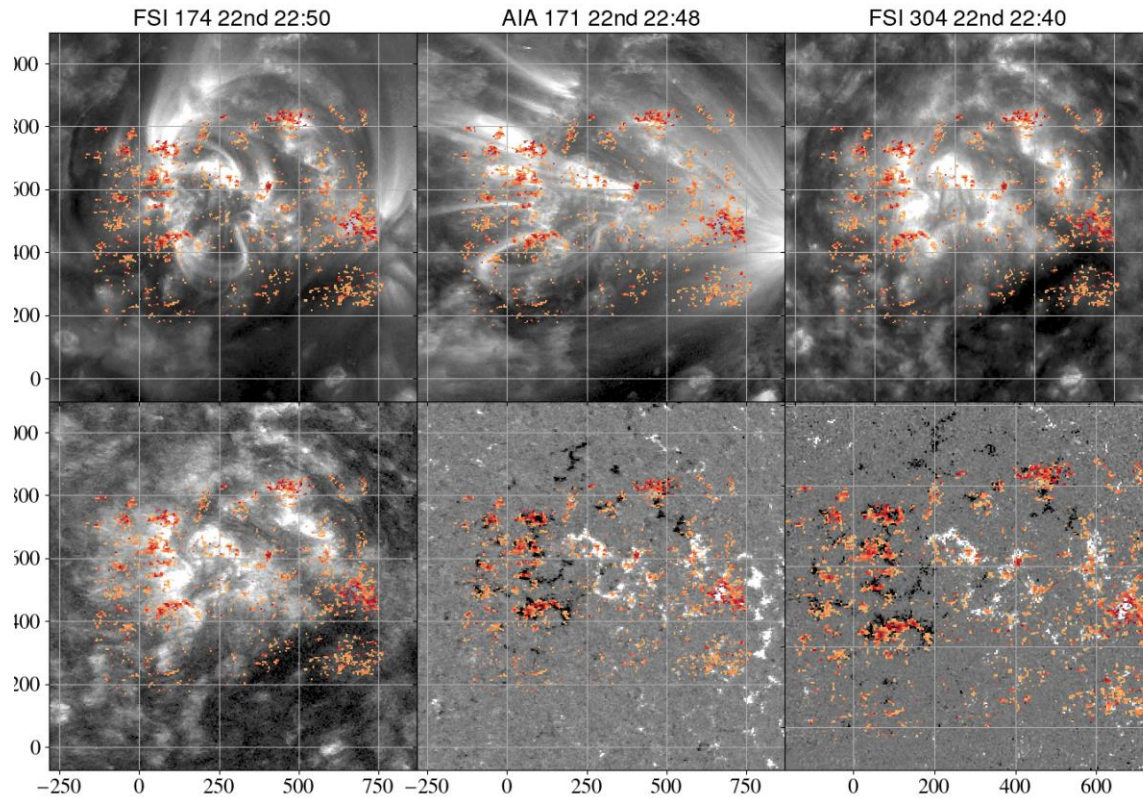


COMPOSITION MAPS (CLEAN RESULTS)

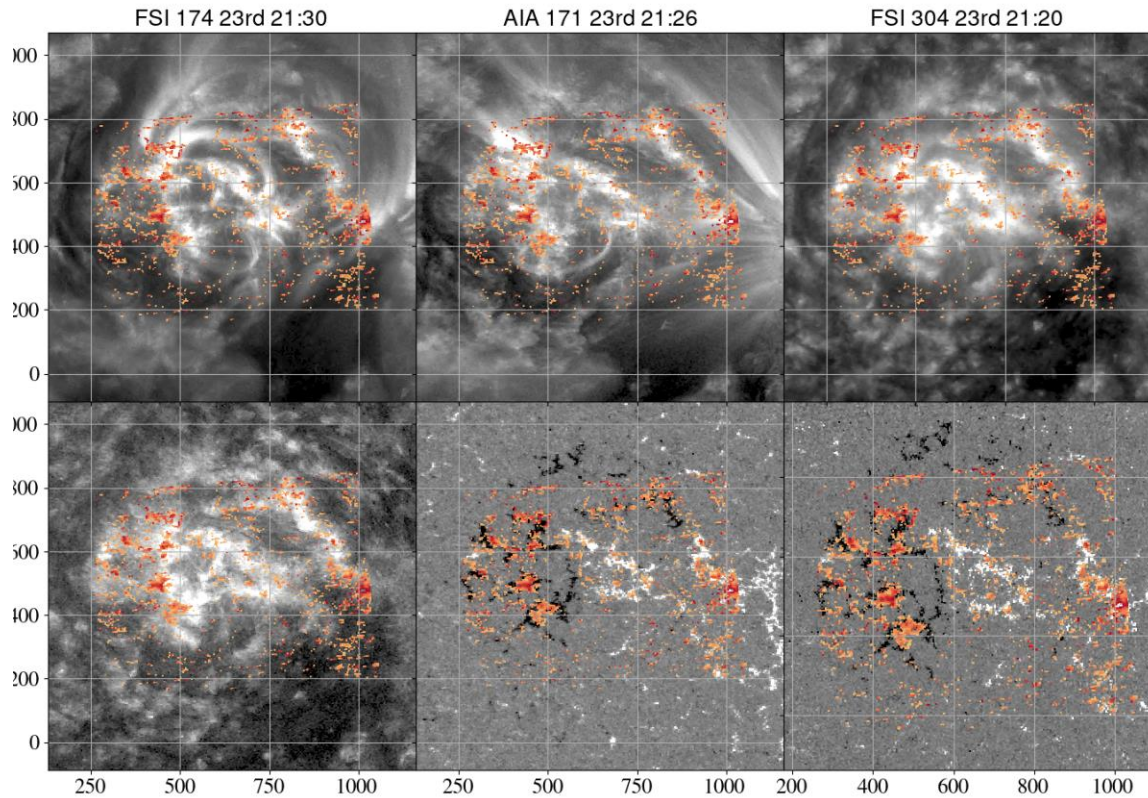


CO-ALIGNING FIP MAPS WITH IMAGES

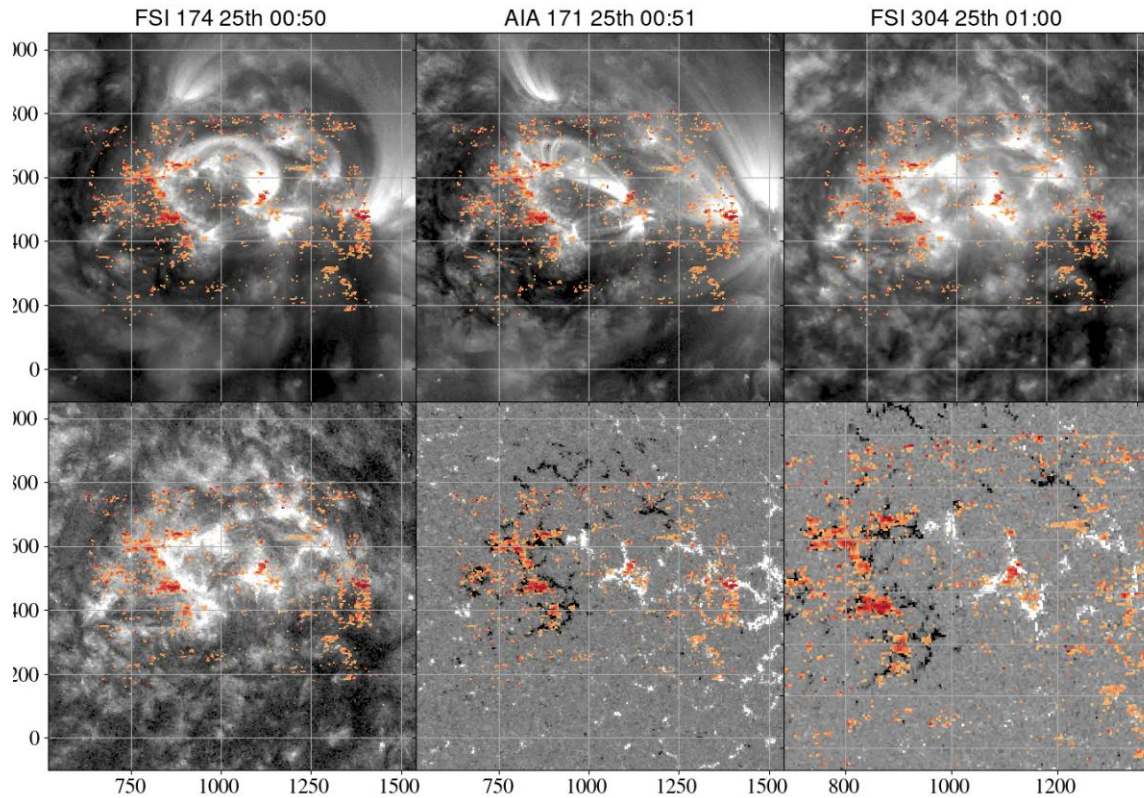




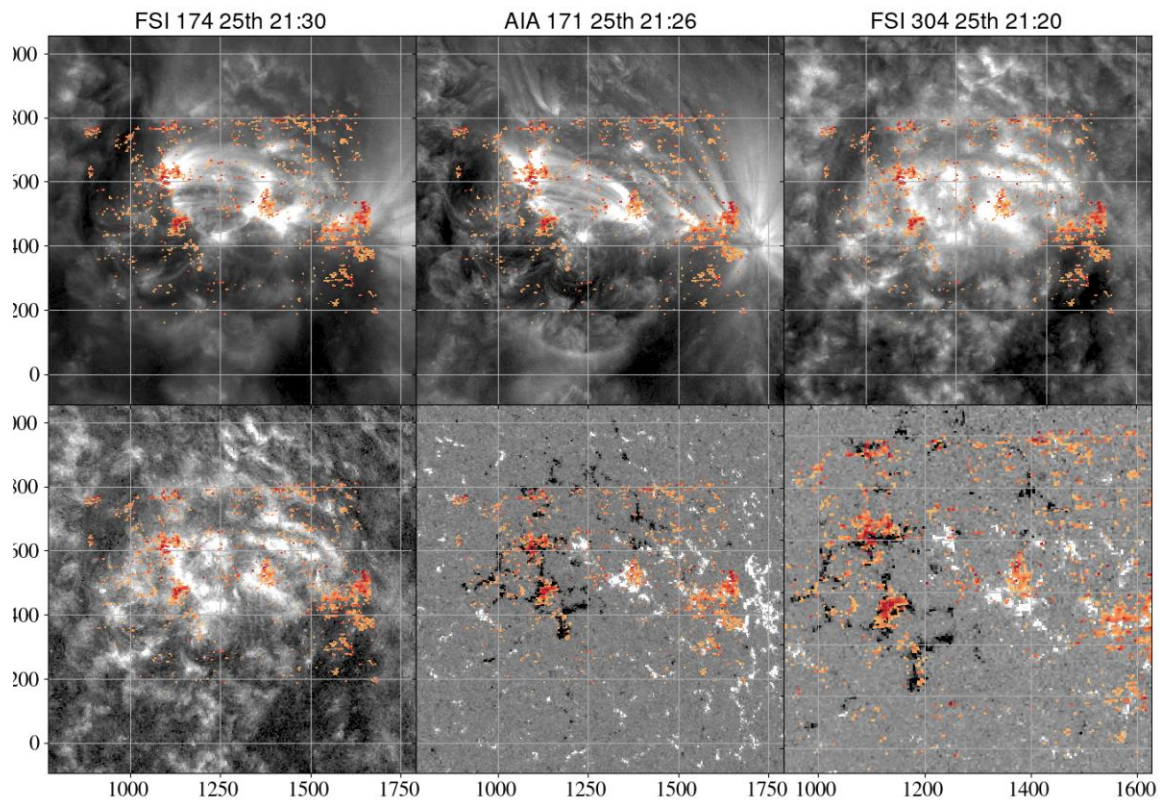
Helioprojective
Coordinates
(Solar Orbiter)



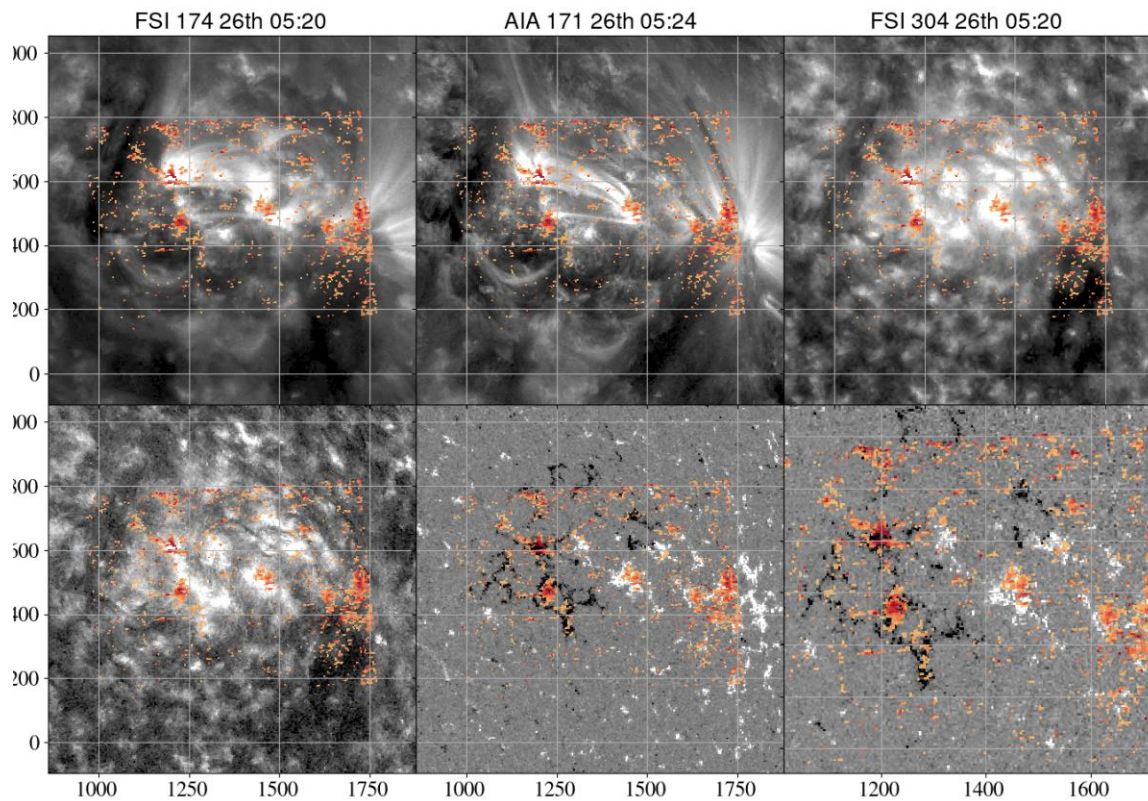
Helioprojective
Coordinates
(Solar Orbiter)



Helioprojective
Coordinates
(Solar Orbiter)



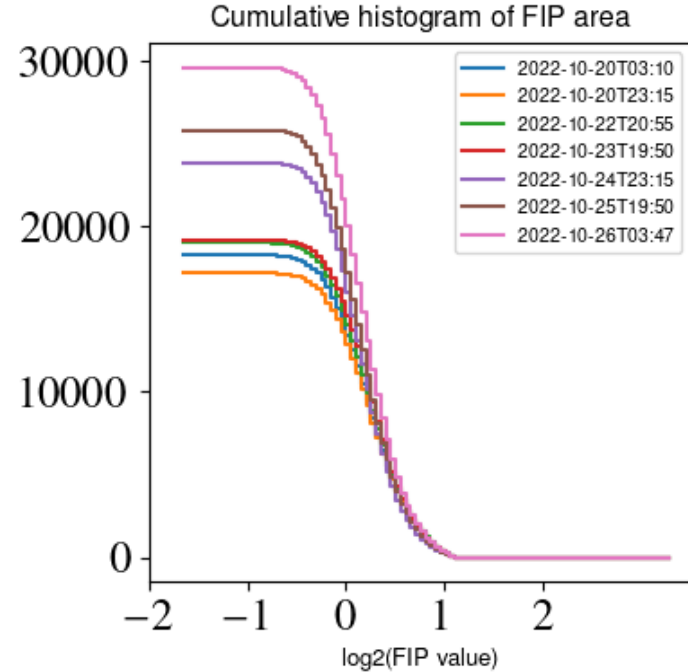
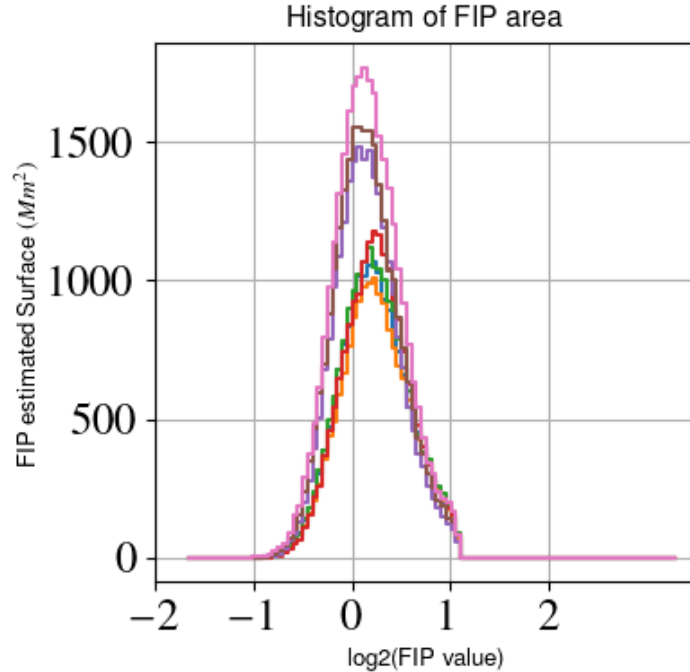
Helioprojective
Coordinates
(Solar Orbiter)



Helioprojective
Coordinates
(Solar Orbiter)

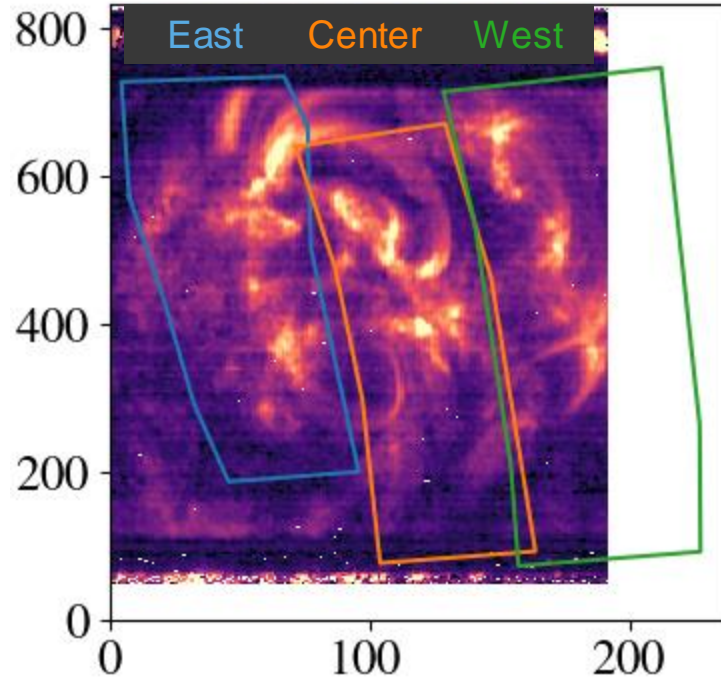
FIP HISTOGRAM

- Histogram of FIP surface
- Total histogram integral \propto distance from the Sun
- A shift from FIP=1 in part because low snr pixels have been eliminated



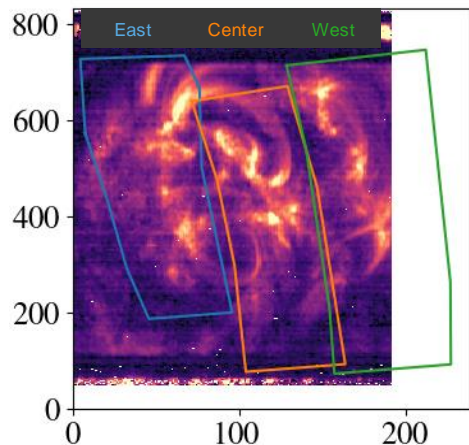
LOCAL ANALYSIS

- Selecting 3 distinct regions based on the loop footpoint sets



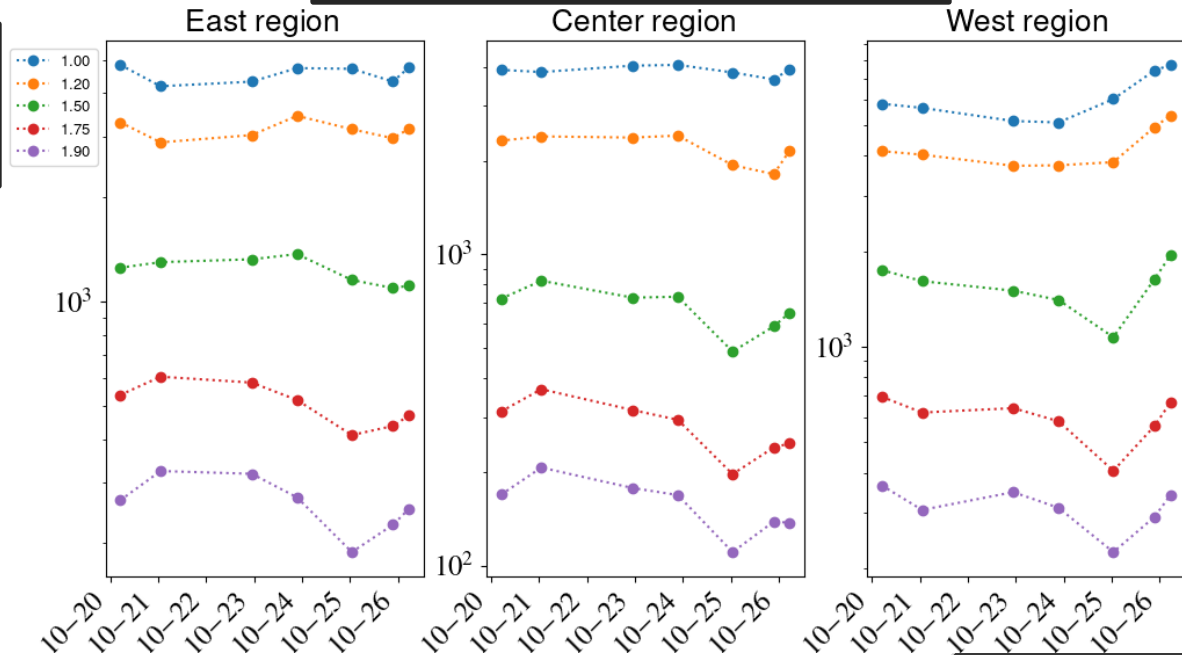
LOCAL ANALYSIS

Area (Mm^2) evolution with time for pixels above some FIP bias values



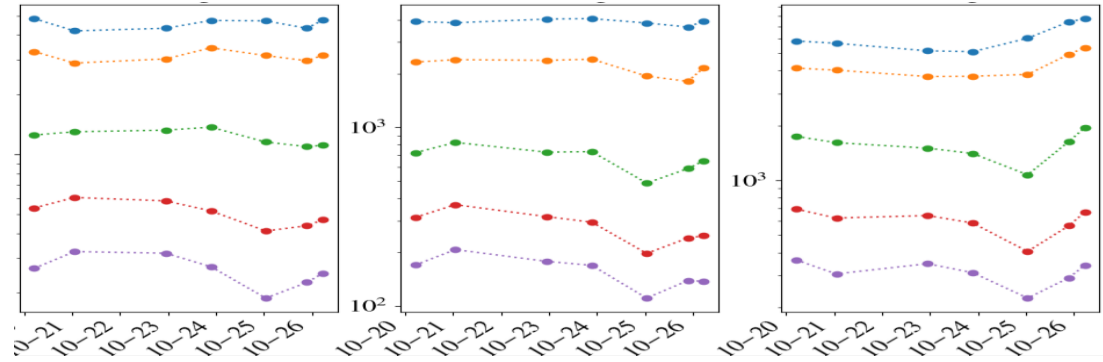
- High FIP bias increase variation around 25-10
- Increase of FIP bias above 1 in the west region
- The overall high FIP bias is increased in the closed loops regions (East, Center) between 21 and 23

FIP bias

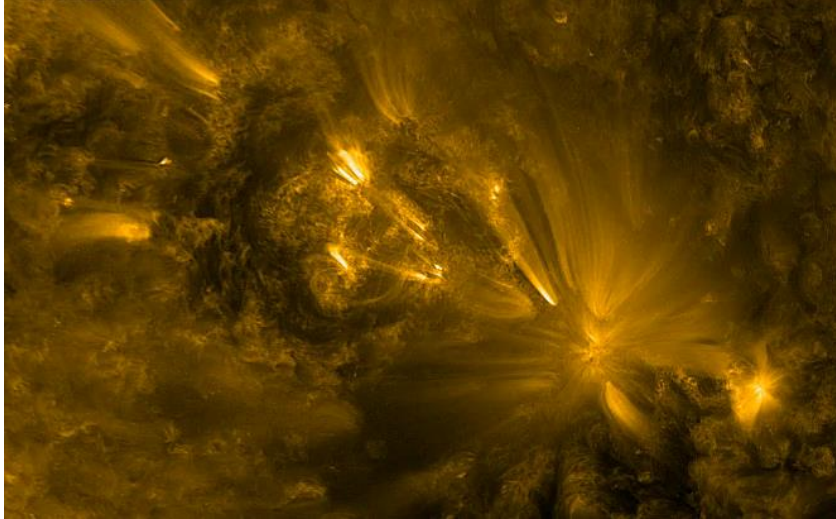


CONCLUSION

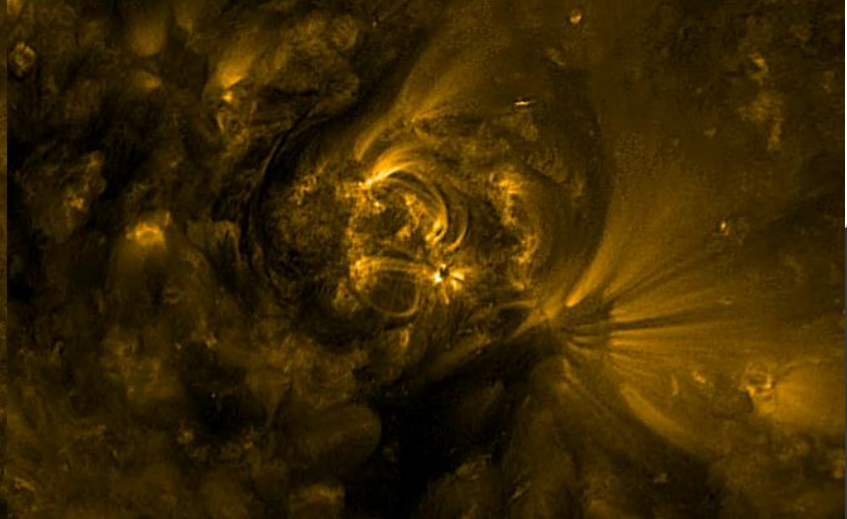
- Current Hypothesis:
Strong change in the
magnetic structure
between October 24 and
25.



AIA 171 2022-10-23T23:59:33.349



EUI FSI 174 2022-10-23T23:20:55.295



WHAT NEXT...

- We are going to analyze Hinode /EIS observations and include them for a coverage of compositions in the mid corona. (Observations available starting from 20-10-2024)
- Comparing sulfur abundance with the theoretical predications under different magnetic configurations.
- Using the magnetogram for magnetic extrapolations

- SAFFRON will be applied for the other observation campaigns. 10-2023, 04-2024 including in-situ measurements from SO, PSP.

